1 **Title: In vitro inhibition of the CFTR ion channel in the *Macaca mulatta* cervix thickens cervical mucus**

2 **Running Title:** CFTR inhibition thickens cervical mucus

3 **Authorship:** Rachel J. Looney[1], Mackenzie Roberts MPH[1], Matthew Markovetz PhD[2], Rachelle Godiah

4 MPH[1], Shan Yao M.D[1], Kirsti Golgotiu[3], Shuhao Wei[1], Chris Cellucci[1], Leo Han M.D. MPH[1,4]

5 **Affiliations:**

6 [1]Division of Reproductive and Developmental Sciences, Oregon National Primate Research Center,

7 Beaverton, OR, USA

8 [2]Marsico Lung Institute, University of North Carolina, Chapel Hill, NC, USA

9 [3]Department of Biomedical Engineering, Oregon Health and Science University, Portland, OR, USA

10 [4]Department of Obstetrics and Gynecology, Oregon Health and Science University, Portland, OR, USA

11 **Summary Sentence**: Inhibition of CFTR, a key epithelial ion channel in primary endocervical cells leads to

12 dehydrated, thickened mucus production in vitro

13 **Key Words:** CFTR, Cervix, Mucus, Fertility, Inh-172, ASL, PTMR

14 **Word Count:** 4679

Funding: Bill & Melinda Gates Foundation [INV-024195], Cystic Fibrosis Foundation [MARKOV22I0], and Oregon National Primate Research Center [P51OD011092].

Corresponding Author:
Leo Han
Oregon National Primate Research Center
505 NW 185th Ave Rm 2116 Beaverton OR 97006
hanl@ohsu.edu

Abstract

Cervical mucus changes throughout the menstrual cycle in response to hormonal fluctuations, regulating access of sperm and pathogens to the reproductive tract. CFTR is an anion channel that plays a critical role in mediating epithelial mucus secretions. Primary endocervical cells obtained from rhesus macaques *Macaca mulatta* were cultured using conditional reprogramming and treated with vehicle controls or CFTR inhibitors. In order to measure changes in hydration and viscosity of secreted mucus, we adapted two airway mucus assays, airway surface liquid and particle-tracking microrheology, for our endocervical culture system. Endocervical cells treated with CFTR inhibitors demonstrated dehydrated, thicker mucus secretions compared to controls in both assay outputs. Our studies suggest that CFTR may be an important mediator of fertility changes and provide experimental evidence for the infertility phenotype seen in women with cystic fibrosis. Additionally, assays developed in these studies provide new endpoints for assessing cervical mucus changes in vitro.

27 **Introduction**

28 Epithelial cells, lining the endocervical canal, control sperm and pathogen entry into the female
29 reproductive tract through changes in cervical mucus secretion. Over the course of the menstrual cycle,
30 fluctuations in ovarian sex-steroids, estradiol (E2) and progesterone (P4), regulate the biophysical
31 properties of secreted mucus[1,2]. When E2 levels peak during the ovulation window, cervical mucus
32 increases in quantity and hydration, and decreases in viscosity, creating a permeable gel that allows
33 sperm to move through the cervix and into the upper tract. Under the influence of P4, following
34 ovulation, cervical mucus increases in concentration, becomes more viscous, and subsequently blocks
35 sperm from entering the reproductive tract [3].

36 The mucus produced by the cervix is a heterogenous mixture of water, mucin and non-mucin
37 proteins, lipids, carbohydrates, and ions. Outside the cervix, other epithelia, including the lung, GI tract,
38 and eye, also produce mucus that maintain organ health and functions. Mucins and proteins found in
39 mucus are retained across organ systems [4]. The Cystic Fibrosis Transmembrane Conductance Regulator
40 (CFTR) ion channel has been shown to be a critical regulator of mucus characteristics in all mucus
41 secreting epithelia. Mutations in the CFTR gene lead to dysfunctional channel activity and the autosomal
42 recessive disease, cystic fibrosis (CF). CF is characterized by systemically thickened mucus secretions that
43 can cause multi-organ dysfunction in the airway, GI tract, and reproductive tract. In the female
44 reproductive tract, CF is notable for thickened endocervical mucus as well as sub-fertile and infertile
45 phenotypes [5,6].

46 The CFTR channel moves chloride and bicarbonate (ions) into the lumen, promoting hydration
47 and the thinning of mucus through two primary mechanisms (Figure 1). First, CFTR maintains an ionic
48 gradient for water to move osmotically [7]. A second channel, the epithelial sodium channel (ENaC),
49 moves sodium into the cell, from the lumen. Thus, increased CFTR activity coupled with decreased ENaC,
50 results in net sodium and chloride ion retention in the lumen and increased water movement to the

51 lumen, with the end result of hydrating mucus and increasing viscosity. Conversely, decreased CFTR
52 activity and/or increased ENaC activity will have the opposite effect of removing salt from the lumen and
53 dehydrating mucus. The second mechanism specifically relates to the critical role CFTR plays in mucin
54 protein unfolding. Large mucin glycoproteins are tightly packaged intracellularly before their release. This
55 is accomplished by storing mucins in secretory granules with low pH and high amounts of cations (e.g.,
56 calcium) to shield the negatively charged carbohydrate-rich ends from themselves while they are stored.
57 Upon release, the higher luminal pH from CFTR secreted bicarbonate, as well as the presence of other
58 luminal anions remove these cations resulting in the immediate expansion and unfolding of the mucins
59 by as much as 500 to 1000-fold in size. In their expanded form, the now "opened" mucin branches are
60 fully exposed and ready to bind water [8]. Thus, when CFTR is dysfunctional, mucins are also unable to
61 fully expand and bind water, leading to the high density, low hydration, and high viscosity mucus seen in
62 CF [9].

63 Our prior studies demonstrated that CFTR in the cervix is both functionally and hormonally
64 regulated [10]. While these findings may suggest that CFTR plays a role in regulating mucus changes in
65 the cervix, CFTR inhibition of endocervical cells and its effect on mucosal thickness and hydration has yet
66 to be demonstrated in an experimental model. Further elucidating the contribution of CFTR in cervical
67 mucus regulation would more precisely define its potential as a target for both fertility and contraceptive
68 studies in the cervix. However, in vitro models for studying endocervical mucus secretion lack
69 experimental endpoints for measuring mucus changes in response to perturbation experiments. To
70 overcome this limitation, we adapted from airway studies of mucus, airway surface liquid (ASL), as a
71 method for measuring mucus hydration in vitro. In vitro ASL correlates tightly to interfacial hydration in
72 vivo [11–13](Figure 2A). ASL in normal airway epithelia [11,14] is lost in CF cells due to mucosal
73 dehydration [15] and can be restored in mutant cell lines with novel CFTR modulator therapies [13,16].
74 While ASL can be directly measured using confocal microscopy in the XZ axis [11], ASL can also be

assessed by measuring the edge-concave meniscus formed under brightfield microscopy that allows 96-well experimental measurement and replication [12](Figure 2B). This measurement of ASL and can also then be used for high-throughput studies of CFTR modulator therapies [16].

While ASL is a measure of liquid-ion transport functionality, it does not provide a direct readout of the biophysical status of the mucus in the lumen. Multiple studies have shown that mucus concentration is the primary driver of aberrant biophysical properties (i.e. viscoelasticity) observed in CF [17,18]. This has been demonstrated with classical rheometric and microscale techniques relevant to the biophysics experienced by sperm within mucus, generally termed particle tracking microrheology (PTMR). PTMR exploits the thermal diffusion of small (~1 µm) fluorescent probes to sense the viscoelasticity of the mucus network. Thus, when volumes of a liquid or gel, are too small for normal rheological instruments, they can be assessed with PTMR.

In this investigation, we adapted both ASL measurements of mucus hydration and PTMR measurements of viscosity to our endocervical cell culture system and used them to assess changes in mucus secretion in response to hormonal treatments and CFTR inhibition. We hypothesized that selectively inhibiting CFTR with several known small molecule inhibitors would result in decreased mucosal hydration, and increased mucus viscosity in vitro.

Methods

Primary cell culture

Rhesus macaque cervical tissue was obtained from the Oregon National Primate Research Center tissue distribution program. Tissue was obtained from animals ranging from 4-15 years with and without history of prior vaginal deliveries. Endocervical epithelia were scalpel separated from the cervical stroma, enzymatically digested, and cultured using conditionally reprogramming conditions as previously described [19]. Expanded cells were passaged at 80% and placed onto HTS Transwell® 96-well

98 and 12-well Permeable Polyester (PET) Supports (0. 4 μm)(Corning, New York) in a serum-free media
99 (ReproLife CX Lifeline Cell Technology, Frederick, Maryland), supplemented with 1M calcium chloride
100 and 10nM E2 and taken to an air-liquid interface (ALI).

101 *Airway surface Liquid*

102 We used transepithelial electrical resistance (TEERs) to determine when cells were ready for
103 experimentation, as TEER levels assess tight junction integrity, cellular polarization and
104 differentiation[20]. After 10-14 days at an air-liquid interface (ALI), when TEER>300 Ω*cm^2, we
105 performed the airway surface liquid assay (ASL) on treatment naïve cells[19]. For ASL, we adapted an
106 assay variation used for high-throughput screening (HTS) in human bronchial epithelial (HBE) cultures
107 that measures the cellularity ability to resorb excess saline added to the apical (mucus) side of ALI
108 culture [16]. Both the rate and magnitude of change to the ASL layer, as the cells try to return the
109 overlying ASL to homeostasis, reflect the underlying mucus secretion and resorption properties of the
110 epithelia. We developed two different versions of the resorption assay. In a version similar to the
111 previously published HTS, phosphate-buffered saline (PBS; 8 μL per well) (Thermo-Fisher Scientific) was
112 added to the apical surface, forming a concave meniscus, and images were taken using brightfield
113 microscopy (2x PlanApoλ NA 0.10 magnification, BZ-X Series, Keyence, Itasca, Illinois). We additionally
114 assessed these changes using an apical addition of 8 μL per well of 100 mM mannitol in PBS. Mannitol is
115 a sugar alcohol that demonstrates osmotic based expansion of ASL in HBE cells and has been studied in
116 clinical trials as potential treatment for CF lung disease [21,22]. We used this combined method of
117 assessing ASL (mannitol+ PBS) as we found that it more robustly defined changes between controls and
118 treatment in ASL studies [23]. Images were taken pre-treatment, immediately post-treatment (0 hours),
119 24, 48, 72, and 96 hours.

120 Following image acquisition, we used custom FIJI [24] scripts to automatically calculate the
121 change in fluid meniscus. The scripts use pixel thresholding to determine the size of the meniscus by
122 measuring the annulus; the annulus is the area of dark fluid meniscus that emanates from the edge of
123 the well to the lighter center region (Figure 2B). This area increases with greater apical hydration and
124 decreases with reduced hydration. The metrics were reported as magnitude change from baseline
125 (time=0 hours) in downstream analysis and statistics. More negative values correspond to greater
126 reduction in the meniscus from the 0Hr time point (time of apical application of PBS). Thus, larger
127 change in meniscal reduction indicates increased dehydration of the cell. As part of our custom scripts,
128 we additionally adjusted for overlying artifacts (i.e. overlaying cellular mucus or debris) in the cell
129 cultures using thresholding, and automatic identification of outliers based on a pre-determined 95%
130 confidence interval. Using the 96-well plate, treatment conditions were repeated using two different
131 plates to account for edge effects with a total of either 48 or 96 wells per condition. Experiments
132 represent at least three or more unique primary cell lines. We used cells between passage two and five.
133 *Particle Tracking Microrheology*
134 To use PTMR for measuring viscosity, 1 µm diameter carboxylated FluoSpheres™ (ThermoFisher,
135 Fremont, CA), henceforth referred to as "beads", were added to the lumen of cell cultures. The thermally
136 driven motion of the beads was tracked to determine the viscoelastic properties of the luminal mucus.
137 Bead motion was recorded for 10s at a rate of 60 frames/s using a 40x air objective on a Zeiss AxioVert
138 A1 Fluorescent microscope (Zeiss, Jena, Germany). Individual bead trajectories were measured
139 automatically using a custom Python program that uses TrackPy [25] for bead localization and tracking.
140 Bead motion was converted into mean squared displacements (MSD) and complex viscosity (η^*) values
141 in accordance with the mathematics described previously [25,26].
142 *CFTR Inhibition*

143 We used two different small molecule CFTR inhibitors: Inh-172 (5 or 10μM) or GlyH-101 (5μM)
144 (MilliporeSigma, Burlington, Vermont)[27]. Inh-172, a thiazolidinone-class CFTR inhibitor, binds inside
145 the channel pore near a transmembrane helix, stabilizing the closed channel conformation, and
146 producing a CFTR mutant like phenotype in inhibited cells[28,29]. GlyH-101 is a glycine hydrazide-class
147 inhibitor that also binds to the membrane-spanning pore region, blocking the channel. Both inhibitors
148 were chosen because they are widely used for CFTR inhibition experiments, do not affect cell viability at
149 effective concentrations, and their mechanism of action and channel specificity are well
150 documented[28–31]. Treatment was applied to the basolateral compartment of the Transwell® every
151 other day.

152 *Statistics*

153 One-way ANOVA was administered using SAS statistical software (Cary, NC). A general linear
154 model testing least squares means for effect was generated and p-values less than 0.05 were considered
155 significant. "N" was denoted as the number of primary cell cultures used for 96-well experiments.
156 Magnitude or reduction in the meniscus from baseline are expressed at means ± SEM.

157 **Results**

158 *Airway Surface Liquid Baseline Assays*

159 We began by demonstrating the ability of our assay to measure changes in apical hydration using
160 mannitol only treatments [32]. Cells were treated with vehicle or mannitol (100mM and 300mM) in PBS
161 (8 μL) applied apically on day 1. Mannitol treated cultures demonstrated persistently elevated ASL
162 meniscus measurements at all time points ($p<.05$, Figure 3). This effect was dose dependent with
163 increased ASL at 300 mM compared to 100 mM (Figure 3).

164 We also sought to demonstrate that ASL measurements responded to hormonal treatment of
165 mucus. Our prior studies demonstrate that conditionally reprogrammed endocervical cells maintain
166 estrogen receptor (ER) and progesterone receptor (PGR) expression and hormonal sensitivity[19,33].

167 Clinically, E2 peaks during ovulation and results in thinner, hydrated mucus. During the luteal phase, P4
168 dominates, and mucus becomes thicker and more dehydrated [34,35]. Thus, we would expect E2 to
169 increase ASL relative to control, and P4 to decrease ASL relative to control [3]. To do this, we treated
170 differentiated cells with E2 (10 nM) or E2/P4 (10 – 14 days of 10 nm E2 priming followed by 1nM E2 and
171 100 nM P4) basolaterally and compared the responses to the vehicle only controls [36–38]. Treatment
172 with 10 nM E2 resulted in greater ASL hydration when compared to the control condition ($p<0.001$)
173 (Figure 4A). Similarly, treatment with 100nM P4 resulted in greater reduction in ASL than 10 nM E2 at
174 every time point ($P<0.05$) (Figure 4B).

175 *ASL response to CFTR Inhibition*

176 10μM Inh-172 resulted in statistically significant ASL dehydration by 48, 72, and 96 hours
177 ($p<0.01$), while 5μM GlyH-101 had a smaller but still significant dehydration effect ($p<0.05$), compared to
178 the control condition (Figure 5A, 5B). Using mannitol in conjunction with PBS amplified the dehydration
179 response across all time points by up to three-fold compared to PBS alone. (Figure 5B).

180 *PTMR response to CFTR- inhibition*

181 The reduction of ASL volume by Inh-172 was visually notable (Figure 5C), resulting in increased
182 mucus concentration and, therefore, an increase in mucus viscoelasticity. This was quantified by PTMR,
183 which demonstrated decreased bead diffusion three-fold, resulting in visually smaller diffusive
184 trajectories (Figure 6). Accordingly, mucus viscoelasticity increased significantly after Inh-172 treatment
185 from 0.15 Pa·s to 0.48 Pa·s in n=6 cultures ($p<0.01$)(Figure 7) and had a more uniform viscosity than
186 untreated controls.

187 **Discussion**

188 Using two different phenotypic assays measuring mucus properties, we demonstrate that
189 inhibition of CFTR in vitro changes secreted mucus by endocervical epithelial cells. Specifically, our
190 results are consistent with the *clinical* findings that mucus is more hydrated in response to E2,

191 dehydrated when exposed to P4, and that CFTR inhibition results in abnormal, dehydrated, thickened
192 mucus secretions similar to that seen in cystic fibrosis [6]. Combined with prior studies that demonstrate
193 the hormonal regulation of CFTR during the menstrual cycle, these findings further support the integral
194 role of CFTR in endocervical mucus changes.

195 Additionally, this study translates two assays, airway surface liquid (ASL) and particle tracking
196 microrheology (PTMR), into endocervical mucus studies [12,25]. New to endocervical mucus studies,
197 these assays provide experimental endpoints that directly reflect mucus changes secreted by cultures,
198 correlated to biophysical properties of mucus itself. ASL, in particular, has potentially high experimental
199 utility as it has been both well validated in mechanistic studies of mucus regulation and used in a high-
200 throughput fashion for drug screening [16]. PTMR is a useful technique for this study for two reasons: it
201 operates and measures forces at the same scale as sperm in the cervical mucus environment, and it has
202 been shown that there is a strong correlation between in vitro mucus models and in vivo mucus in the
203 airway [25]. Uniquely, the reduced ciliary activity/presence in the conditionally reprogrammed
204 endocervical cell cultures allows for PTMR to be performed *in situ*, further increasing its utility here.

205 Both assays provide potential endpoints for future studies of mucus in vitro. One challenging
206 characteristic of studying endocervical mucus is the lack of valid small animal models. Classic
207 mammalian models, such as rodents, are poor options for studying cervical mucus changes or lower
208 tract fertility as they lack a mucus secreting endocervix and sperm is ejaculated directly into the uterus
209 [39]. In larger mammalian models, experimental rigor is challenging due to biological variability, semi-
210 quantitative nature of mucus appraisal, and invasiveness for mucus collection. An in vitro model provides
211 a tool for mechanistic studies to determine the key regulators of mucus changes such as CFTR, but also a
212 platform for drug discovery. With recent advances in primary cell culture such as conditional
213 reprogramming, there is further potential for study of genetic differences and personalization of drugs
214 response [40].

215 Our previous studies demonstrate that CFTR is a hormonally regulated ion channel with E2 (mid
216 cycle) conditions upregulating CFTR gene expression and, conversely, P4 (luteal) conditions
217 downregulating CFTR expression [10]. In CF, the CFTR gene mutation produces a defective channel,
218 resulting in thick, viscous cervical mucus. Prior to the drug discovery and development of small
219 molecules that modulate mutant CFTR function, women with CF had known infertility/subfertility
220 phenotypes that were largely attributed to these mucus changes, preventing sperm penetration [41]. In
221 our study, we used inhibitors to mimic CFTR mutation, recapitulating this phenotype in vitro. Thus, our
222 study is one of the first to experimentally confirm the relationship of CFTR inhibition and mucus changes
223 using loss of function experiments in vitro. Additionally, it provides evidence that CFTR is likely a critical
224 mediator of mucus changes in normal menstrual cycles.

225 Our in vitro study does not fully recapitulate either tissue level characteristics of epithelial
226 biology nor the full content of mucus secretions produced in vivo. However, the conditionally
227 reprogrammed platform used in this investigation provides a robust model where we can investigate
228 epithelial changes under multiple treatment conditions, while evaluating mucus production and quality.
229 We have previously demonstrated in proteomic studies, high similarity between the mucus produced in
230 vitro using this cellular system to in vivo mucus [10,19,42], and epithelial only cell models have been
231 used to high success in disease investigations and drug discovery in other mucosal systems [40,43].

232 The extent to which CFTR is responsible for mucus changes in the cervix is not fully quantified by
233 our studies. CFTR, while a critical channel with a well-known mutated human phenotype, is part of a
234 large ecosystem of ion channels. There are other ion channels, such as the epithelial sodium channel
235 (ENaC) that are hormonally active and may be involved in mucus hydration [44]. Investigating the relative
236 contributions of different ion channels in mucosal hydration using our endpoints could provide a more
237 comprehensive understanding of female fertility and the development of nonhormonal drug therapies.

238 Additionally, future studies might develop our findings further by examining the effect of CFTR inhibition
239 on fertility and mucus consistency and hydration in vivo using a whole animal model.

240 **Conclusion**

241 Cervical mucus produced by the epithelia in the endocervix is a hormonally induced regulator of
242 female fertility. In this investigation we validate and employ two different techniques, ASL and PTMR, to
243 measure the viscosity and hydration of endocervical cell mucus. We determined that the inhibition of
244 CFTR using small molecule inhibitors results in significant dehydration and increased viscosity of cervical
245 mucus in vitro. These findings are consistent with the physiology seen clinically and predicted by
246 molecular studies of CFTR gene expression.

247 **Author contribution statement**

248 RL: performed experiments, analyzed data, wrote paper
249 MR: performed experiments, analyzed data, wrote paper
250 MM: performed experiments, analyzed data, wrote paper
251 RG: performed experiments, analyzed data, wrote paper
252 SY: performed experiments, analyzed data
253 KG: performed experiments, analyzed data, wrote paper
254 SW: performed experiments, analyzed data
255 CC: performed experiments, analyzed data
256 LH: conceived the study, performed experiments, analyzed data and wrote the paper

257 **Acknowledgements**

258 This work was supported, in whole or in part, by the Bill & Melinda Gates Foundation [INV-
259 024195]. Under the grant conditions of the Foundation, a Creative Commons Attribution 4.0 Generic
260 License has already been assigned to the Author Accepted Manuscript version that might arise from this
261 submission.

Funding

This work was funded by the Bill & Melinda Gates Foundation [INV-024195], Cystic Fibrosis Foundation [MARKOV22I0], and Oregon National Primate Research Center [P51OD011092].

Declaration of interest

There is no conflict of interest to report.

Data Availability Statement

The data underlying this article will be shared on reasonable request to the corresponding author.

References

[1] Moghissi KS, Syner FN, Evans TN. A composite picture of the menstrual cycle. Am J Obstet Gynecol 1972; 114:405–418.

[2] Najmabadi S, Schliep KC, Simonsen SE, Porucznik CA, Egger MJ, Stanford JB. Cervical mucus patterns and the fertile window in women without known subfertility: a pooled analysis of three cohorts. Hum Reprod 2021; 36:1784–1795.

[3] Moghissi KS. The function of the cervix in fertility. Fertil Steril 1972; 23:295–306.

[4] Thornton DJ, Rousseau K, McGuckin MA. Structure and Function of the Polymeric Mucins in Airways Mucus. Annu Rev Physiol 2008; 70:459–486.

[5] Anthony E, Oppenheimer, Case AL, Esterly JR, Rothberg RM. Cervical mucus in cystic fibrosis: A possible cause of infertility. American Journal of Obstetrics and Gynecology 1970; 108:673–674.

[6] Kopito LE, Kosasky HJ, Shwachman H. Water and electrolytes in cervical mucus from patients with cystic fibrosis. Fertil Steril 1973; 24:512–516.

[7] Saint-Criq V, Gray MA. Role of CFTR in epithelial physiology. Cell Mol Life Sci 2017; 74:93–115.

[8] Muchekehu RW, Quinton PM. A new role for bicarbonate secretion in cervico-uterine mucus release. J Physiol 2010; 588:2329–2342.

286 [9] Clunes MT, Boucher RC. Cystic fibrosis: the mechanisms of pathogenesis of an inherited lung
287 disorder. Drug Discovery Today: Disease Mechanisms 2007; 4:63–72.
288 [10] Han L, Roberts M, Luo A, Wei S, Slayden OD, Macdonald KD. Functional evaluation of the cystic
289 fibrosis transmembrane conductance regulator in the endocervix. Biology of Reproduction 2022;
290 107:732–740.
291 [11] Tarran R, Boucher RC. Thin-film measurements of airway surface liquid volume/composition and
292 mucus transport rates in vitro. Methods Mol Med 2002; 70:479–492.
293 [12] Harvey PR, Tarran R, Garoff S, Myerburg MM. Measurement of the Airway Surface Liquid Volume
294 with Simple Light Refraction Microscopy. Am J Respir Cell Mol Biol 2011; 45:592–599.
295 [13] Haq IJ, Gray MA, Garnett JP, Ward C, Brodlie M. Airway surface liquid homeostasis in cystic fibrosis:
296 pathophysiology and therapeutic targets. Thorax 2016; 71:284–287.
297 [14] Myerburg MM, Butterworth MB, McKenna EE, Peters KW, Frizzell RA, Kleyman TR, Pilewski JM.
298 Airway surface liquid volume regulates ENaC by altering the serine protease-protease inhibitor
299 balance: a mechanism for sodium hyperabsorption in cystic fibrosis. J Biol Chem 2006; 281:27942–
300 27949.
301 [15] Matsui H, Grubb BR, Tarran R, Randell SH, Gatzy JT, Davis CW, Boucher RC. Evidence for periciliary
302 liquid layer depletion, not abnormal ion composition, in the pathogenesis of cystic fibrosis airways
303 disease. Cell 1998; 95:1005–1015.
304 [16] Berg A, Hallowell S, Tibbetts M, Beasley C, Brown-Phillips T, Healy A, Pustilnik L, Doyonnas R, Pregel
305 M. High-Throughput Surface Liquid Absorption and Secretion Assays to Identify F508del CFTR
306 Correctors Using Patient Primary Airway Epithelial Cultures. SLAS Discovery 2019; 24:724–737.
307 [17] Button B, Cai L-H, Ehre C, Kesimer M, Hill DB, Sheehan JK, Boucher RC, Rubinstein M. A periciliary
308 brush promotes the lung health by separating the mucus layer from airway epithelia. Science 2012;
309 337:937–941.

310 [18] Hill DB, Long RF, Kissner WJ, Atieh E, Garbarine IC, Markovetz MR, Fontana NC, Christy M,
311 Habibpour M, Tarran R, Forest MG, Boucher RC, et al. Pathological mucus and impaired mucus
312 clearance in cystic fibrosis patients result from increased concentration, not altered pH. Eur Respir J
313 2018; 52:1801297.
314 [19] Han L, Andrews W, Wong K, Jensen JT. Conditionally reprogrammed macaque endocervical cells
315 retain steroid receptor expression and produce mucus. Biology of Reproduction 2020; 102:1191–
316 1202.
317 [20] Jaques A, Daviskas E, Turton JA, McKay K, Cooper P, Stirling RG, Robertson CF, Bye PTP, LeSouëf PN,
318 Shadbolt B, Anderson SD, Charlton B. Inhaled Mannitol Improves Lung Function in Cystic Fibrosis.
319 Chest 2008; 133:1388–1396.
320 [21] Keyrouz SG, Dhar R, Diringer MN. Variation in Osmotic Response to Sustained Mannitol
321 Administration. Neurocrit Care 2008; 9:204–209.
322 [22] Locke LW, Myerburg MM, Markovetz MR, Parker RS, Weber L, Czachowski MR, Harding TJ, Brown
323 SL, Nero JA, Pilewski JM, Corcoran TE. Quantitative imaging of airway liquid absorption in cystic
324 fibrosis. Eur Respir J 2014; 44:675–684.
325 [23] Schindelin J, Arganda-Carreras I, Frise E, Kaynig V, Longair M, Pietzsch T, Preibisch S, Rueden C,
326 Saalfeld S, Schmid B, Tinevez J-Y, White DJ, et al. Fiji: an open-source platform for biological-image
327 analysis. Nat Methods 2012; 9:676–682.
328 [24] Myerburg MM, Harvey PR, Heidrich EM, Pilewski JM, Butterworth MB. Acute regulation of the
329 epithelial sodium channel in airway epithelia by proteases and trafficking. Am J Respir Cell Mol Biol
330 2010; 43:712–719.
331 [25] Nussey S, Whitehead S. Endocrinology: An Integrated Approach. Oxford: BIOS Scientific Publishers;
332 2001.

333 [26] Hombach-Klonisch S, Kehlen A, Fowler PA, Huppertz B, Jugert JF, Bischoff G, Schlüter E, Buchmann
334 J, Klonisch T. Regulation of functional steroid receptors and ligand-induced responses in
335 telomerase-immortalized human endometrial epithelial cells. Journal of Molecular Endocrinology
336 2005; 34:517–534.
337 [27] Buckner LR, Schust DJ, Ding J, Nagamatsu T, Beatty W, Chang TL, Greene SJ, Lewis ME, Ruiz B,
338 Holman SL, Spagnuolo RA, Pyles RB, et al. Innate immune mediator profiles and their regulation in
339 a novel polarized immortalized epithelial cell model derived from human endocervix. Journal of
340 Reproductive Immunology 2011; 92:8–20.
341 [28] Verkman AS, Synder D, Tradtrantip L, Thiagarajah JR, Anderson MO. CFTR inhibitors. Curr Pharm
342 Des 2013; 19:3529–3541.
343 [29] Markovetz MR, Subramani DB, Kissner WJ, Morrison CB, Garbarine IC, Ghio A, Ramsey KA, Arora H,
344 Kumar P, Nix DB, Kumagai T, Krunkosky TM, et al. Endotracheal tube mucus as a source of airway
345 mucus for rheological study. Am J Physiol Lung Cell Mol Physiol 2019; 317:L498–L509.
346 [30] Hill DB, Vasquez PA, Mellnik J, McKinley SA, Vose A, Mu F, Henderson AG, Donaldson SH, Alexis NE,
347 Boucher RC, Forest MG. A Biophysical Basis for Mucus Solids Concentration as a Candidate
348 Biomarker for Airways Disease. PLOS ONE 2014; 9:e87681.
349 [31] Cunha GR, Sinclair A, Ricke WA, Robboy SJ, Cao M, Baskin LS. Reproductive tract biology: Of mice
350 and men. Differentiation 2019; 110:49–63.
351 [32] Liu X, Krawczyk E, Suprynowicz FA, Palechor-Ceron N, Yuan H, Dakic A, Simic V, Zheng Y-L,
352 Sripadhan P, Chen C, Lu J, Hou T-W, et al. Conditional reprogramming and long-term expansion of
353 normal and tumor cells from human biospecimens. Nat Protoc 2017; 12:439–451.
354 [33] Hodges CA, Palmert MR, Drumm ML. Infertility in Females with Cystic Fibrosis Is Multifactorial:
355 Evidence from Mouse Models. Endocrinology 2008; 149:2790–2797.

356 [34] Park D, Reddy AP, Wilmarth PA, Jensen JT, Han L. Mucus secretions from a conditionally
357 reprogrammed primary endocervical cell culture. F S Sci 2022; 3:159–165.
358 [35] Gentzsch M, Boyles SE, Cheluvaraju C, Chaudhry IG, Quinney NL, Cho C, Dang H, Liu X, Schlegel R,
359 Randell SH. Pharmacological Rescue of Conditionally Reprogrammed Cystic Fibrosis Bronchial
360 Epithelial Cells. Am J Respir Cell Mol Biol 2017; 56:568–574.
361 [36] Roberts M, Yao S, Wei S, Jensen JT, Han L. Hormonal regulation of non-cystic fibrosis
362 transmembrane conductance regulator ion channels in the endocervix. F S Sci 2023; 4:163–171.

363 **Figure Legends**

364 **Figure 1:** This figure illustrates the relationship between CFTR and ENAc as it pertains to regulating
365 mucus concentration.

366 Alt text: A figure where two ion channels are seen to regulate mucus concentration. The flow of ions can
367 also be seen.

368 **Figure 2:** (A) This figure illustrates the XZ- plane of a Transwell® during an experiment. The apical
369 meniscus view shows the change in meniscus corresponding to CFTR function. (B) This figure
370 demonstrates the image obtained from brightfield microscopy used in ASL studies. The cells can be seen
371 in the center of the field forming a monolayer. The darker outer ring is the meniscus or annulus formed
372 by mucus and PBS on the apical surface of the Transwell®.

373 **Alt text:** (A) A cross-sectional diagram showing an experimental setup of endocervical epithelial cells)
374 within a liquid-filled container. To the right of the container, there are two circular illustrations labeled
375 "Apical Meniscus View." One circle represents a hydrated, "unimpaired" meniscus, while the other
376 shows a dehydrated, "impaired" meniscus. (B) A grayscale circular image resembling a microscope view,
377 featuring concentric rings with distinct boundaries outlined in white. The distance between edge of the
378 well and the lighter region is the annulus.

379 **Figure 3**: Effect of mannitol on ASL hydration. Across all time points (24, 48 hours from administration)
380 mannitol (100 mM and 300 mM) reduced the measured change in meniscus from baseline compared to
381 the control (n=4, P<0.05).
382 **Alt text**: Bar chart showing reduction in meniscus from baseline for various treatment groups over time.
383 **Figure 4**: (A). Effect of E2 on ASL hydration. Across all time points (24, 48, 72, 96 hours from
384 administration) E2 (10 nM) reduced the measured change in meniscus from baseline compared to the
385 control(n=6, P<0.001). (B). Effect of E2 and P4/E2 on ASL hydration. Across all time points (24, 48, 72, 96
386 hours from administration) 100 nM P4 (after E2 priming) increased the measured change in meniscus
387 from baseline as compared E2 only (n=6, P<0.05).
388 **Alt text**: Bar charts showing reduction in meniscus from baseline for various treatment groups over time.
389 **Figure 5**: (A) Effect of InH-172 and GlyH-101 on ASL Hydration. Across time points 48, 72, and 96 hours
390 from administration, 10 μM Inh-172 (n=6) and 5 μM GlyH-101(n=6) increased the measured change in
391 meniscus from baseline compared to the control (P<0.01, P<0.05 respectively). (B) Effect of Inh-172 and
392 Mannitol on ASL Hydration. Across time points 48, 72 and 96 hours from administration, 5 μM Inh-172
393 with 100 mM mannitol (n=6) increased the measured change in meniscus from baseline compared to
394 the control (P<0.05, P<0.01, P<0.01 respectively). (C) Representative images obtained at 0 hr and 96 hr
395 with control and Inh-172. These examples were chosen as visually greater reduction of the meniscus in
396 the Inh-172 condition is seen.
397 **Alt text:** Bar charts showing reduction in meniscus from baseline for various treatment groups over time.
398 Chart A compares three groups, and chart B compares two groups. A collection of four images depicting
399 a single culture well. The dark region represents the meniscus which decreases over time in both
400 conditions.
401 **Figure 6:** Representative bead trajectories after treatment with either DMSO or Inh-172. Treatment with
402 Inh-172 resulted in significantly less bead movement compared to DMSO treatment.

403 **Alt text**: a figure representing the movement of microscopic beads in mucus secreted by cells treated

404 with DMSO (blue) and Inh-172 (red).

405 **Figure 7:** Effect of 10 µM Inh-172 on mucus complex viscosity (η*). Treatment with Inh-172 for 72 hours

406 increased mucus secretion η* ($p<0.01$; $n=6$).

407 **Alt text:** a graph demonstrating the difference between DMSO and Inh-172 on complex viscosity.

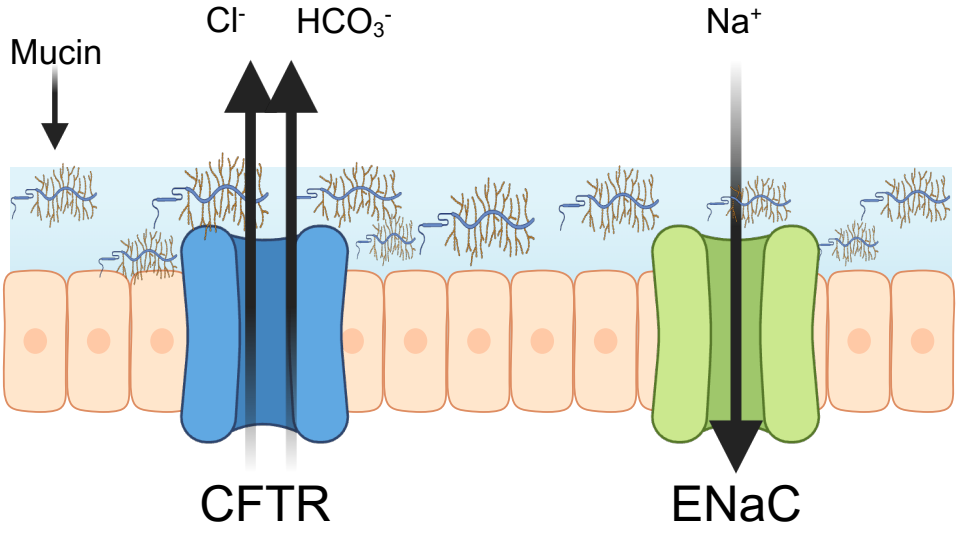
Mucin
Cl-
HCO3-
Na+
CFTR
ENaC

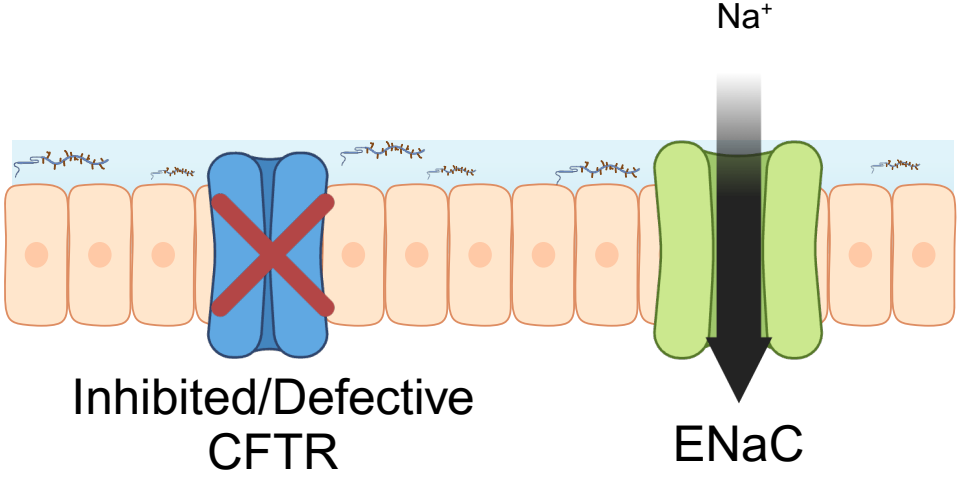
Na+
Inhibited/Defective
CFTR
ENaC

A

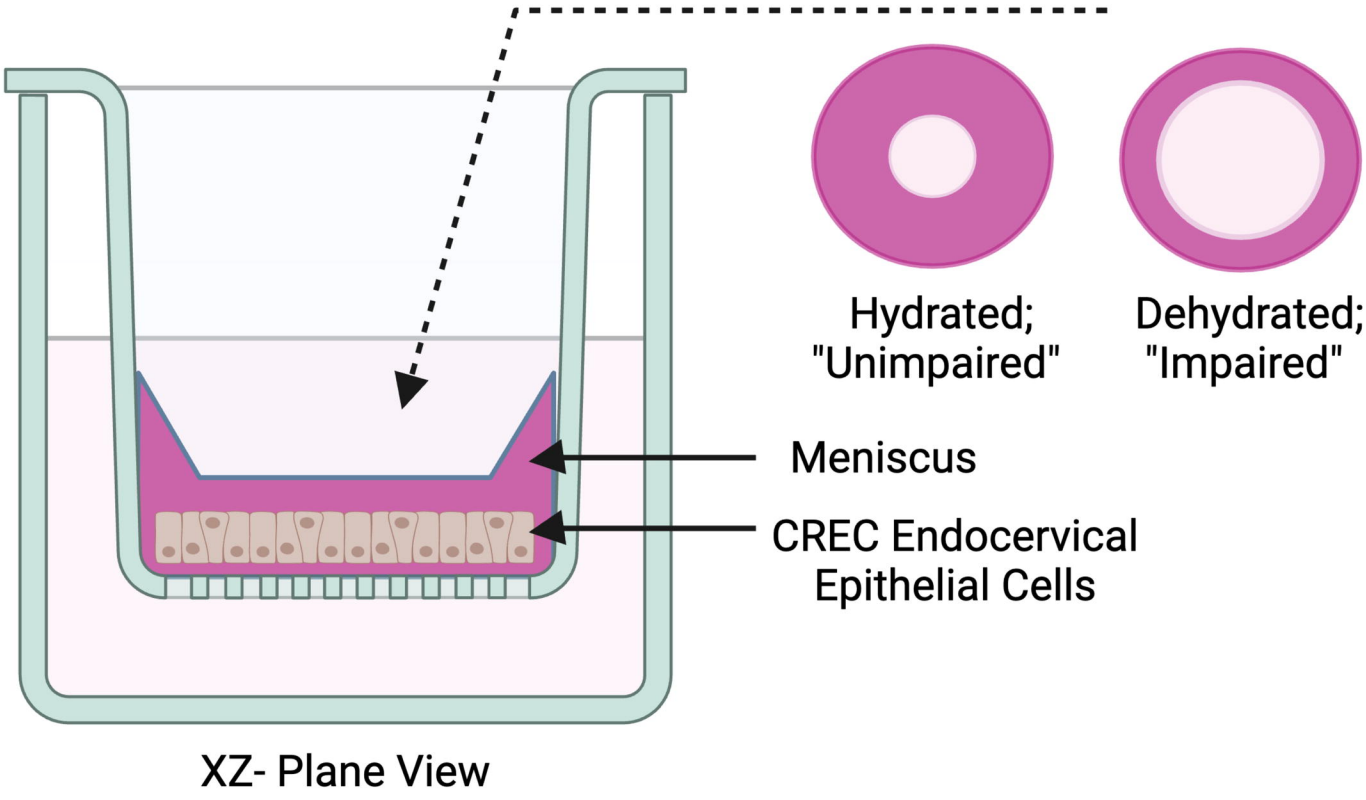
Apical Meniscus View
Hydrated;
"Unimpaired"
Dehydrated;
"Impaired"
Meniscus
CREC Endocervical
Epithelial Cells
XZ- Plane View

B

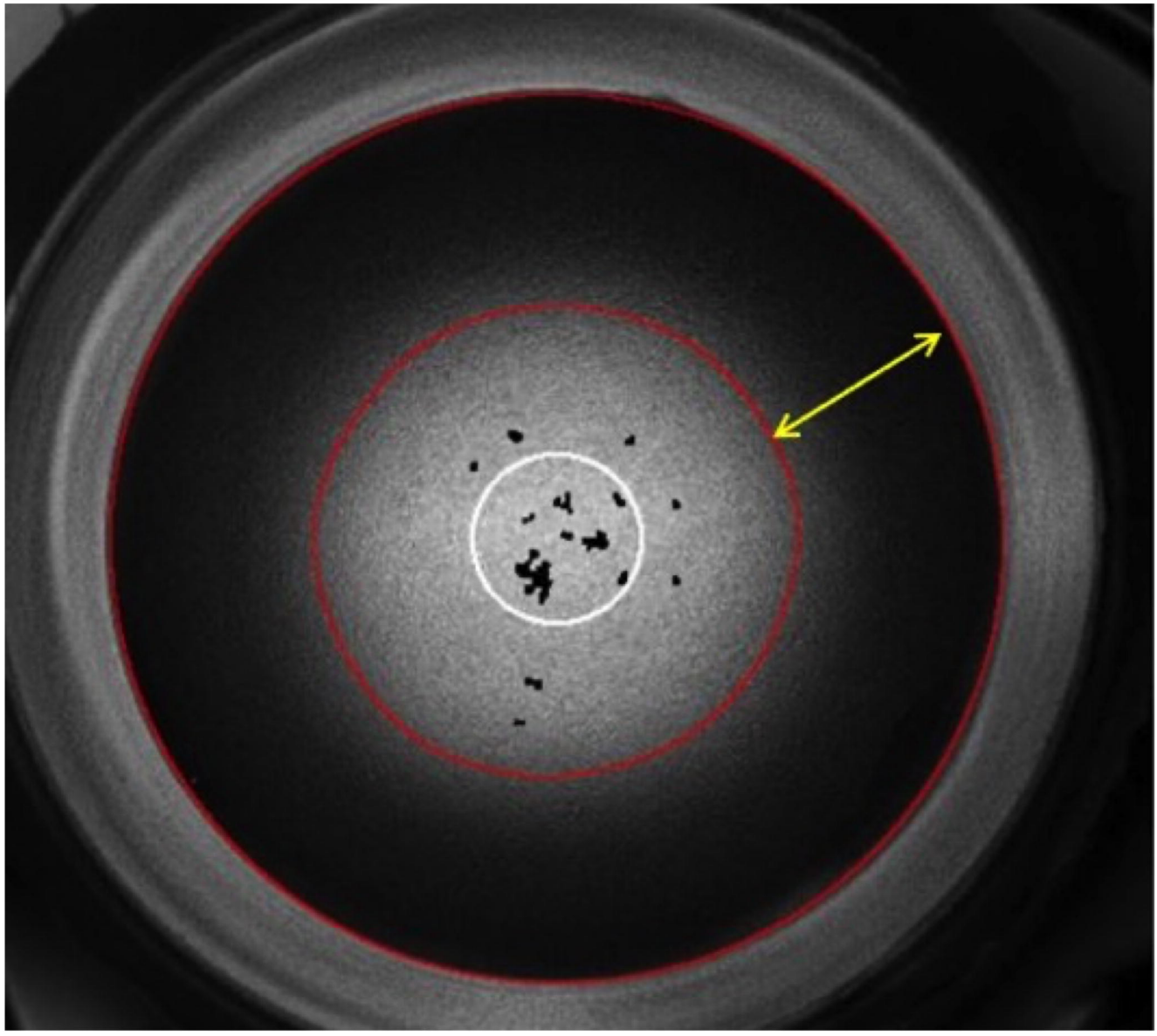

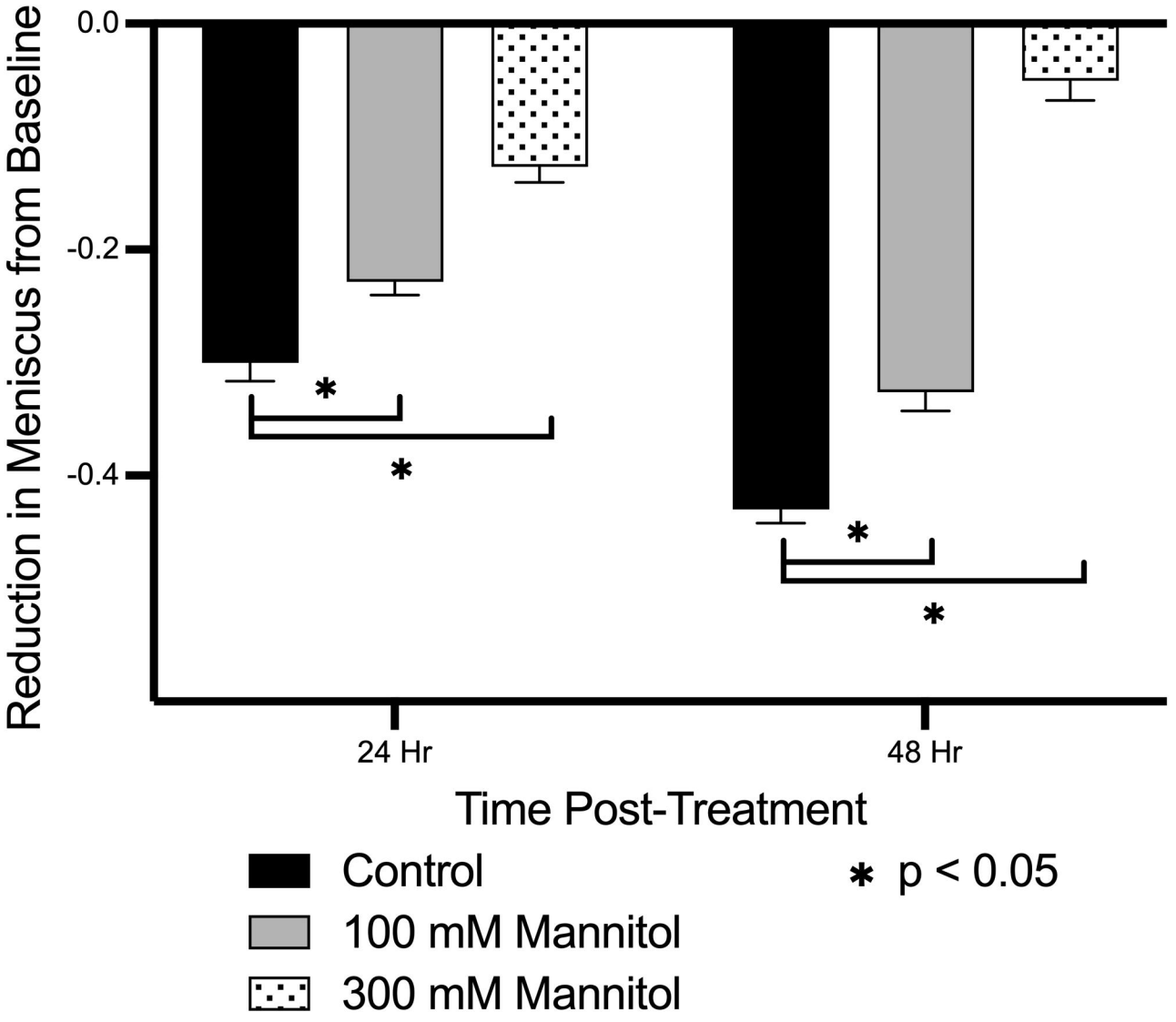
Reduction in Meniscus from Baseline
0.0
-0.2
-0.4
*
*
*
*
24 Hr
48 Hr
Time Post-Treatment
Control
100 mM Mannitol
300 mM Mannitol
* p < 0.05

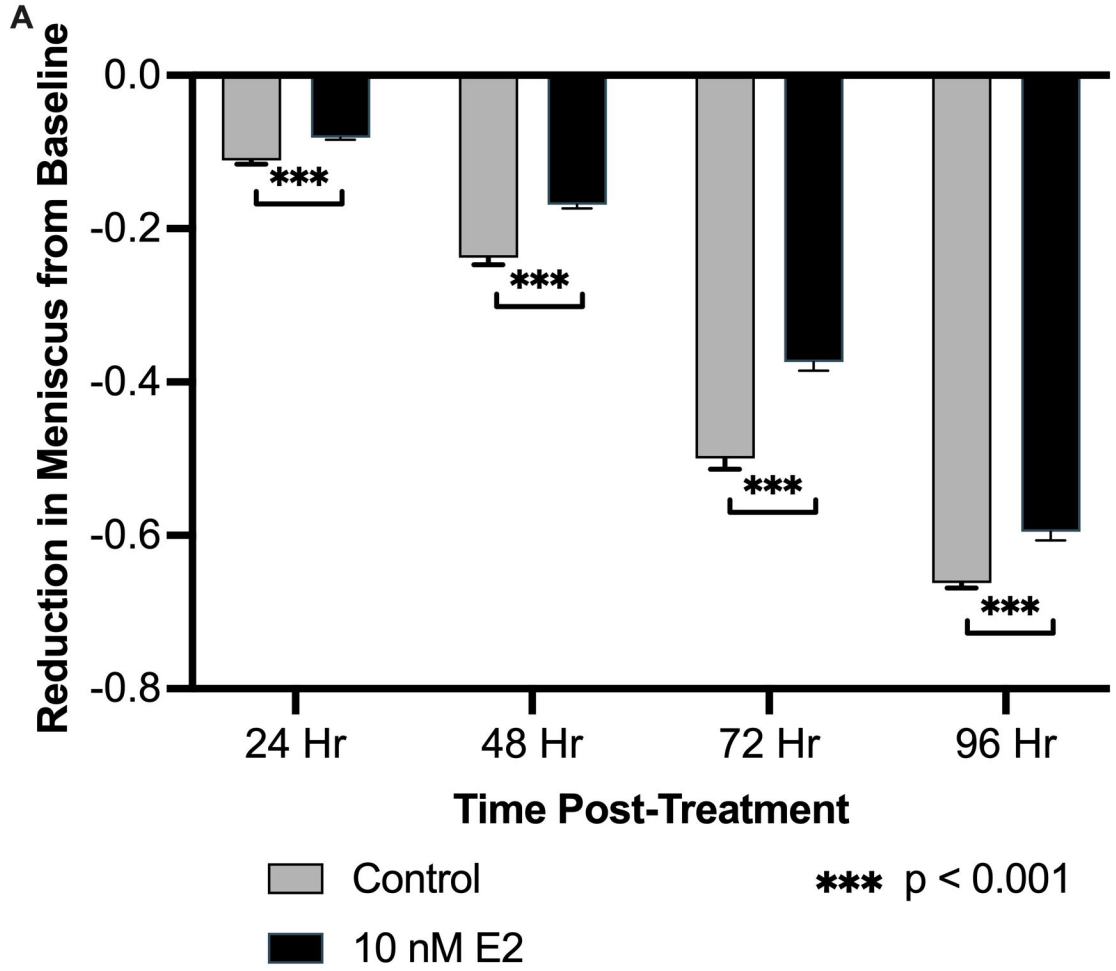
A
Reduction in Meniscus from Baseline
0.0
-0.2
-0.4
-0.6
-0.8
***
***
***
***
24 Hr
48 Hr
72 Hr
96 Hr
Time Post-Treatment
Control
10 nM E2
*** p < 0.001

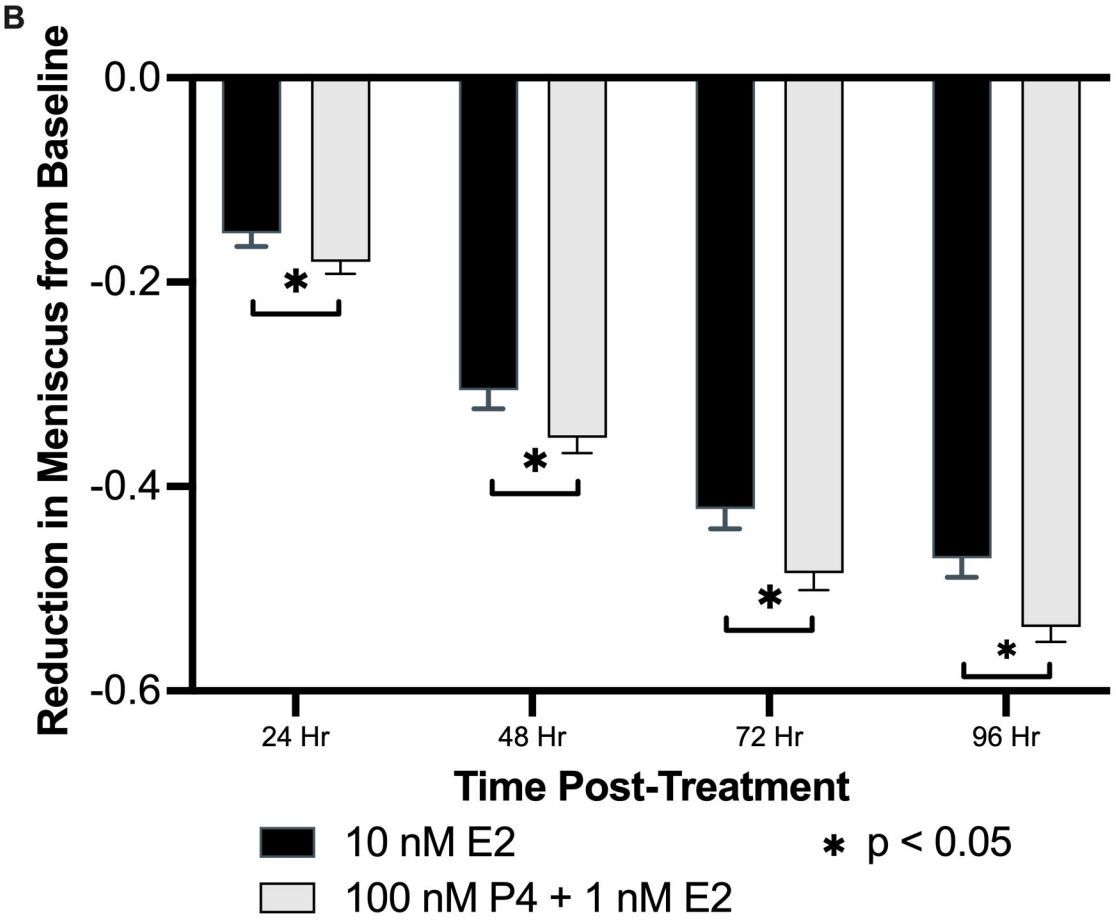
B
Reduction in Meniscus from Baseline
0.0
-0.2
-0.4
-0.6
*
*
*
*
24 Hr
48 Hr
72 Hr
96 Hr
Time Post-Treatment
10 nM E2
100 nM P4 + 1 nM E2
* p < 0.05

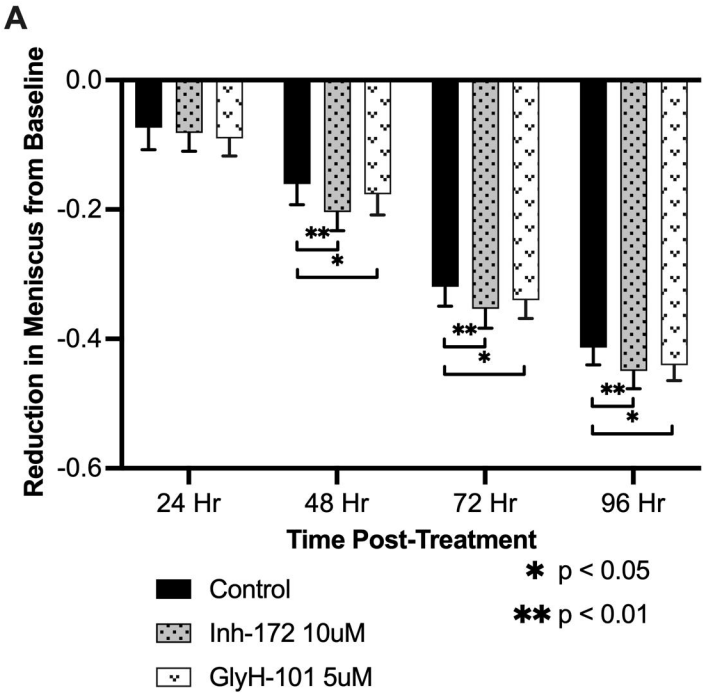
A
Reduction in Meniscus from Baseline
0.0
-0.2
-0.4
-0.6
24 Hr
48 Hr
72 Hr
96 Hr
Time Post-Treatment
Control
Inh-172 10uM
GlyH-101 5uM
* p < 0.05
** p < 0.01

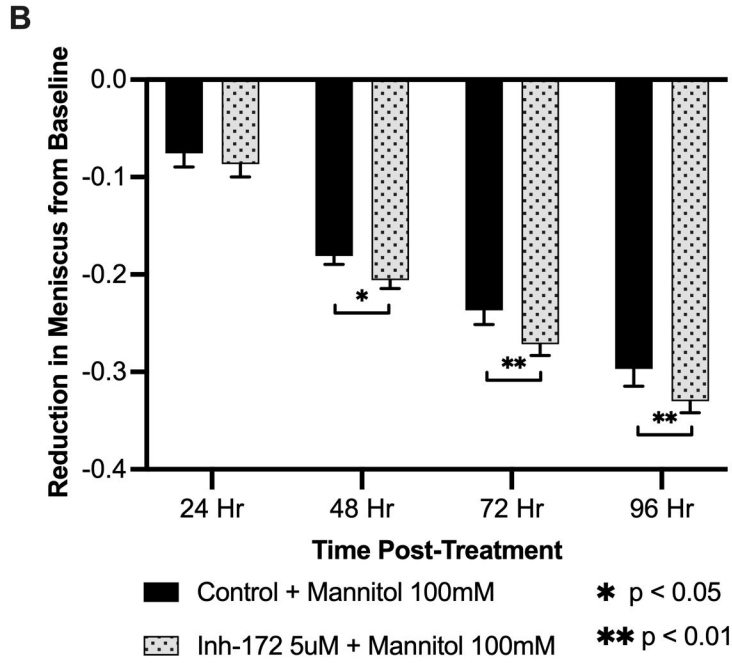
B
Reduction in Meniscus from Baseline
0.0
-0.1
-0.2
-0.3
-0.4
24 Hr
48 Hr
72 Hr
96 Hr
Time Post-Treatment
Control + Mannitol 100mM
Inh-172 5uM + Mannitol 100mM
* p < 0.05
** p < 0.01

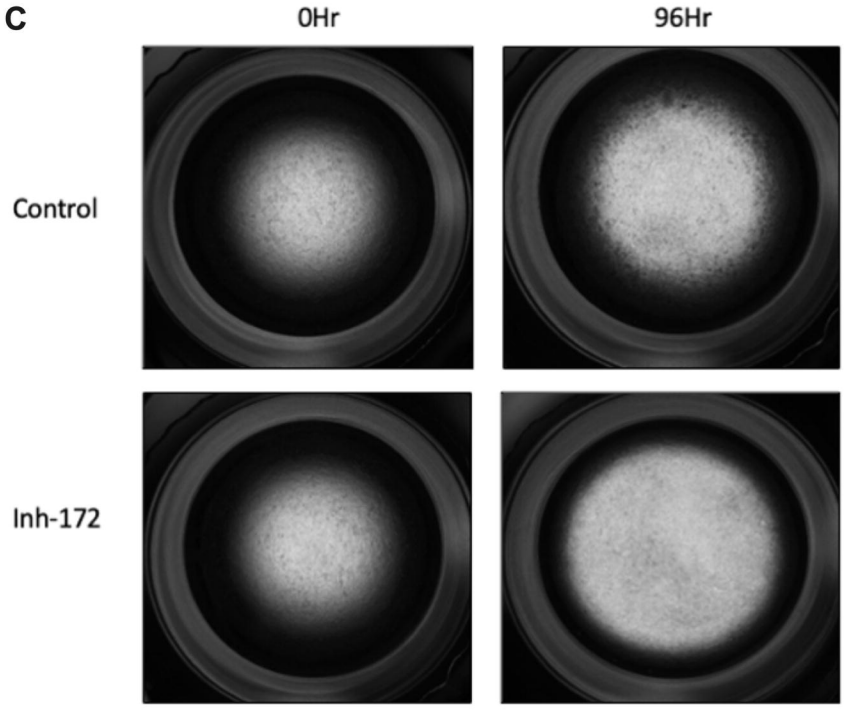
C
0Hr
96Hr
Control
Inh-172

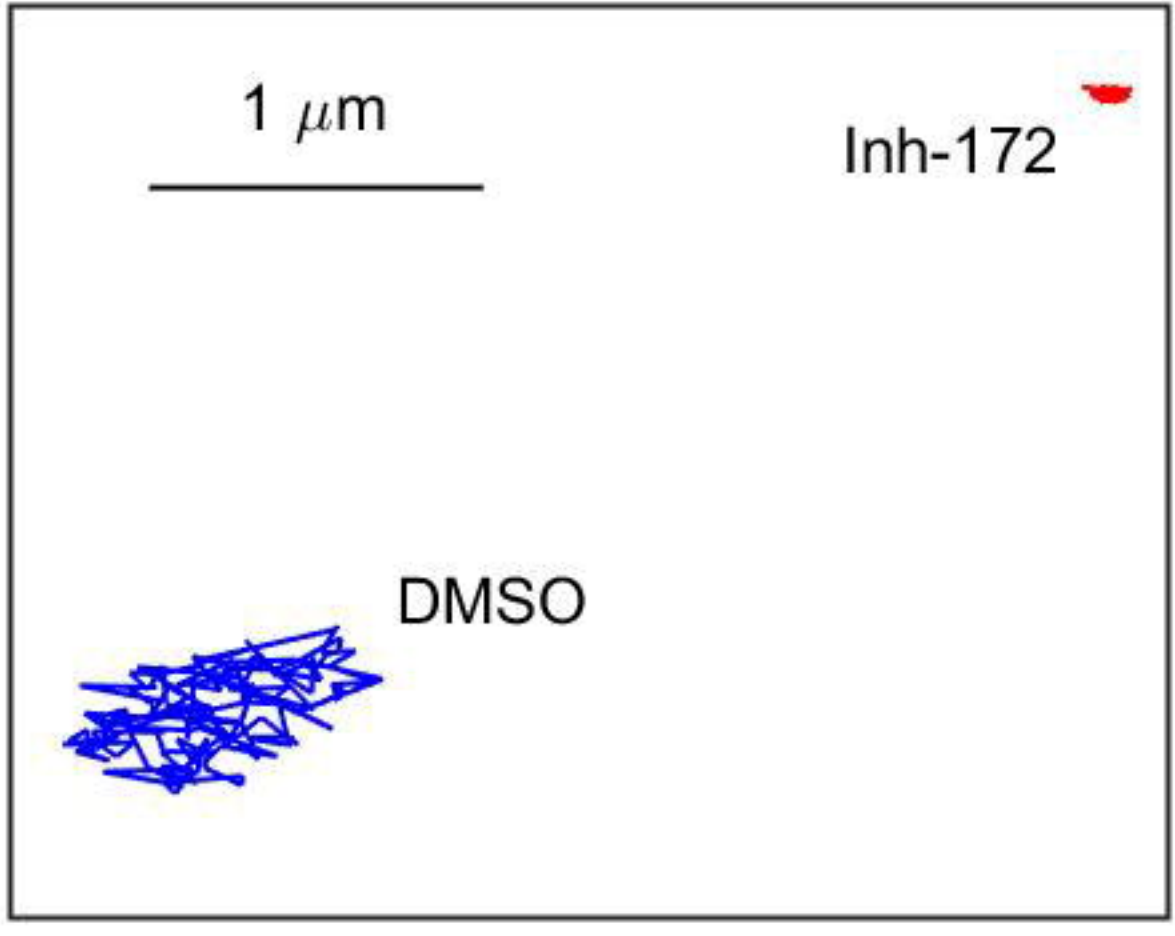
1 μm
Inh-172
DMSO

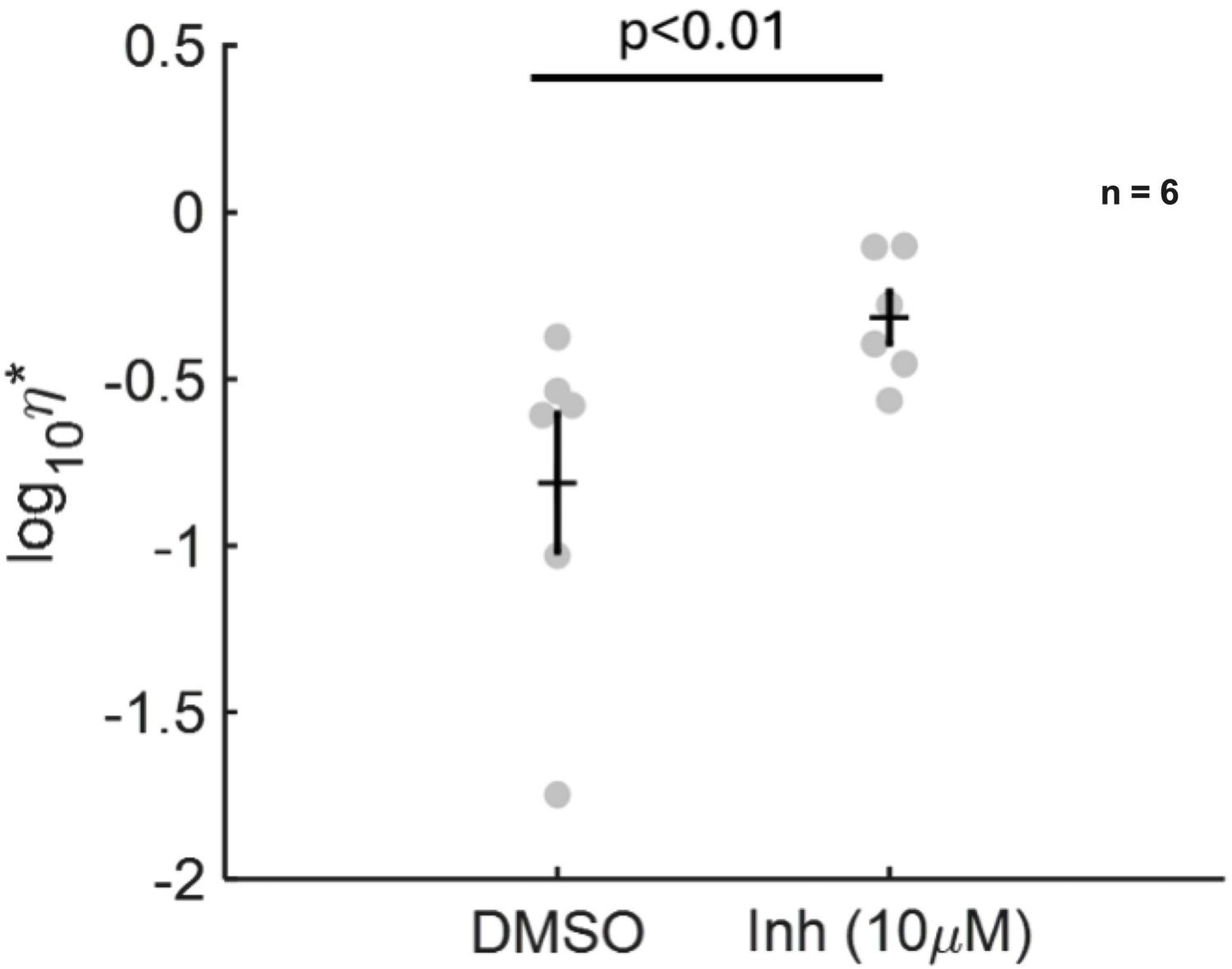
p<0.01
n = 6
0.5
0
-0.5
-1
-1.5
-2
$\log_{10}\eta^*$
DMSO
Inh (10μM)